Electronic Supplementary Material (ESI) for ChemComm.

Supporting Information

Ammonia decomposition mediated at nitrogen vacancy on NaCl-type binary metal nitride supported with transition metal nanoparticles

Masayoshi Miyazaki,[†] Kiya Ogasawara,[†] Yousuke Takekoshi,[†] Kazuki Miyashita,[†] Hitoshi Abe,[‡] Yasuhiro Niwa,[‡] Hideo Hosono*,[†] and Masaaki Kitano,*,[†,§]

[†] *MDX Research Center for Element Strategy, International Research Frontiers Initiative, Tokyo Institute of Technology, 4259 Nagatsuta, Midori-ku, Yokohama 226-8503, Japan*

[‡] *Institute of Materials Structure Science, High Energy Accelerator Research Organization, 1-1, Oho, Tsukuba, Ibaraki 305−0801, Japan*

[§] *Advanced Institute for Materials Research (WPI-AIMR), Tohoku University, Sendai 980-8577, Japan*

Hideo Hosono

E-mail: *hosono@mces.titech.ac.jp* , Tel: +81-45-924-5009,

Masaaki Kitano

E-mail: *kitano.m.aa@m.titech.ac.jp* , Tel: +81-45-924-5191,

1. Experimental

1.1. Sample preparation

The LaN and CeN were synthesized by the nitridation of LaH_3 and CeH_3 as previously reported in the literature.[1] The LaH_3 and CeH_3 were, in turn, prepared by hydrogenation of pieces of La and Ce metal (99.9%, Rare Metallic Co.) under 1.5 MPa of H_2 gas at room temperature for 2 h. LaN and CeN were subsequently prepared from the hydride powders by heating at 600 °C under a N_2 gas flow (10 mL·min^{-1}) for 12 h. Other nitride materials (YN, ZrN, and HfN) were purchased from the Kojundo Chemical Laboratory. CeN with high surface area (CeN-HS) was synthesized via nitridation of a CeH_2 nanopowder made by an arc-evaporation method as previously reported.[2] Nickel-supported catalysts were synthesized by H_2 reduction reactions of mixtures of $Ni(\eta\text{-}C_5H_5)_2$ (98.0%, Tokyo Chemical Industry) and various support materials at 250 °C for 1.5 h.

1.2. Catalytic reactions

Each ammonia decomposition reaction was conducted in a fixed-bed plug-flow silica glass tube reactor at ambient pressure. Each of the prepared catalysts was pretreated by heating under a N_2/H_2 mixed gas flow (N_2:H_2=1:3, 20 mL·min^{-1}) at 500 °C for 1 h. Catalytic performance and stability tests were conducted using 0.1 g catalyst specimens over the range of 360–660 °C in a stream of pure NH_3 gas (25 mL·min^{-1}), corresponding to a weight hourly space velocity (WHSV) of 15,000 $mL_{NH3}·g^{-1}·h^{-1}$. Effluent gases were analyzed with an online gas chromatograph (GC-14A, incorporating a thermal conductivity detector and Porapak OS column, Shimadzu, with He as the carrier gas). The NH_3 conversion was calculated as

$$X_{NH3} = \frac{C_{NH3,\,0} - C_{NH3}}{C_{NH3,0} + C_{NH3}} \quad (1)$$

Where $C_{NH3,0}$ is the concentration of NH_3 in the inlet gas and C_{NH3} is the concentration in the outlet gas. Trials involving ^{15}N-labeled NH_3 gas decomposition were performed at 500 °C over both the Ni/CeN and CeN specimens in a U-shaped quartz glass reactor connected to a closed gas

circulation system. These experiments each employed 75 mg of the catalyst and introduced 4.0 mmol $^{15}NH_3$ (98% isotopic purity).

1.3. Characterization

The crystal structures of the catalysts were examined by acquiring powder X-ray diffraction (XRD) patterns (D2 PHASER, Bruker) employing Cu Kα radiation. To prevent the air exposure of the unstable nitrides (LaN, CeN, and YN), we employed the Ar-sealed XRD holder, which has a broad amorphous diffraction below $\theta = 25°$. H_2-TPD and N_2-TPD analyses were conducted using a BELCAT-A apparatus (MicrotracBEL, Japan). Ni K-edge X-ray adsorption fine structure (XAFS) data were obtained using the synchrotron radiation ring at the PF-12C beamline of the KEK Photon Factory with Si(111) single-crystal monochromators. Brunauer−Emmett−Teller (BET) surface areas were calculated based on N_2 adsorption−desorption isotherms acquired at 77 K using a BELSORP-mini II apparatus (MicrotracBEL).

1.4. Density functional theory calculations

Periodic density functional theory (DFT) calculations based on slab models were performed using the Vienna Ab Initio Simulation Package (VASP) code[3] with the Perdew−Burke−Ernzerhof exchange−correlation functional[4] based on the projector augmented wave (PAW) method.[5,6] The plane-wave basis set was truncated at a kinetic energy of 500 eV and a Monkhorst-Pack k-point grid separation[7] for the Brillouin zone sampling was 3 × 3 × 1 for each surface models . The convergence criteria for structural optimization and energy calculations comprised an SCF tolerance of 1.0×10^{-6} eV per atom, an energy tolerance of 5.0×10^{-5} eV per atom and a maximum force tolerance of 0.05 eV·Å^{-1}. The DFT + U method (DFT plus Hubbard-U parameter) was employed for all DFT calculations.[8] The effective Hubbard-U parameter, that is, U − J, was set to 7.0 eV (Ce) and 4.0 eV (La). The formation Energy of N^{3-} vacancies on each nitride surface was defined as

$$E_f(V_N) = \left\{E(S^d) + 0.5 \times E(N_2)\right\} - E(S^p)$$

Where E(A) represents the total energy of system A and S^d and S^p represent Nitrides and without surface V_N, respectively.

Table

Table S1. Specific surface area of nitrides.

Nitrides	Specific surface area ($m^2 \cdot g^{-1}$)
CeN	3.5
CeN-HS	23.1
LaN	1.9
YN	4.0
ZrN	1.0
HfN	0.1

Table S2. Summary of previously reported Ni-supported catalyst for ammonia decomposition.

Catalysts	Ni content (wt%)	T (°C)	WHSV ($mL g_{cat.}^{-1} h^{-1}$)	Conversion (%)	H_2 production rate ($mmol_{H2} g_{cat.}^{-1} min^{-1}$)	H_2 production rate ($mmol_{H2} g_{Ni}^{-1} min^{-1}$)	Ref.
Ni/CeN-HS	10	500	15000	86.4	14.5	144.6	This work
Ni/CeN	5	500	15000	51.2	8.6	171.4	This work
Ni/LaN	5	500	15000	39.3	6.6	131.6	This work
Ni/YN	5	500	15000	16.7	2.8	55.9	This work
Ni/ZrN	5	500	15000	5.2	0.9	17.4	This work
Ni/HfN	5	500	15000	0.9	0.2	3	This work
$NaNH_2$-Ni-GNP	8	500	60000	-	13.9	173.4	9
Ce-Ni/Al_2O_3	43.4	500	30000	71.9	24.1	55.5	10
La-Ni/Al_2O_3	37.9	500	30000	63.9	21.4	56.5	11
Ni/SBA-15	23.4	500	30000	57	19.1	81.6	12
Ni/MCM-41	7.2	500	30000	26.9	9	125.1	13
Ni/SiO_2	10	500	30000	10.5	3.5	35.2	14
Ni/CNT	2.9	500	30000	9	3	103.9	15
Ni-Ce-Al-O microsphere	-	500	18000	88	17.7	-	16
Ni/h-$BaTiO_{3-x}N_y$	5	500	15000	58	9.7	194.3	17
Ni/CaNH-HS	10	500	15000	91.2	15.3	152.7	18
Ni/Al_2O_3	10	500	15000	20	3.3	33.5	18
Ni/CaO	10	500	15000	16	2.7	26.8	18
Ni/C12A7:e-	7.4	500	15000	13.3	2.2	30.1	18
Ni doped $LiNH_2$/C	5	400	13000	53	7.7	153.8	19

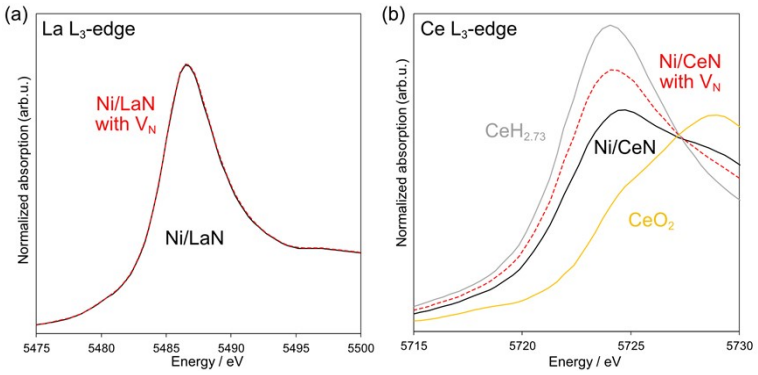

Figures

Figure S1. XANES spectra before and after introduction of V_N for (a) Ni/LaN and (b) Ni/CeN with the references. $CeH_{2.73}$ was prepared by the hydrogenation of metal Ce under 1 MPa H_2 at room temperature. The chemical composition of prepared hydride was determined to be $CeH_{2.73}$ by the XRD patterns in previous study.[20]

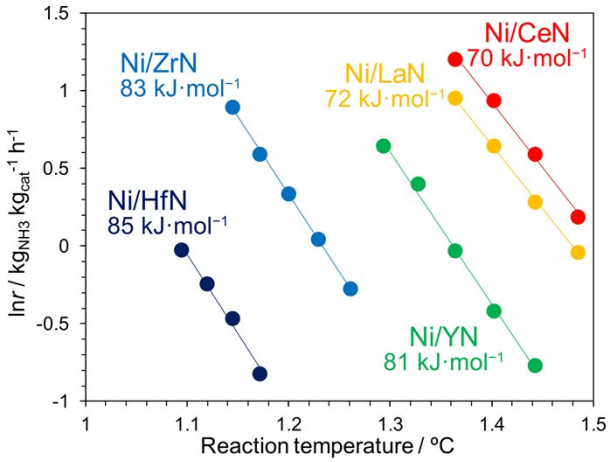

Figure S2. Arrhenius plots for ammonia decomposition over Ni/TMN (TM = La, Ce, Y, Zr or Hf) below 30% NH_3 conversion.

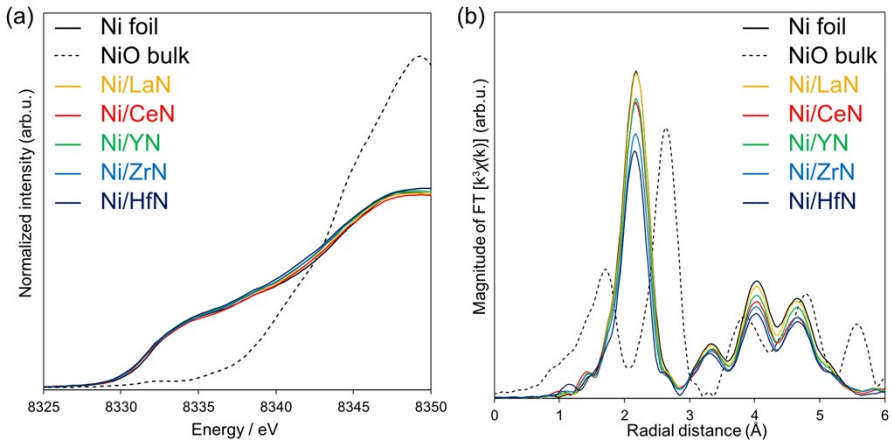

Figure S3. (a) Ni K-edge XANES spectra of Ni/nitrides along with Ni and NiO as references. (b) Fourier transform of k^3-weighted EXAFS oscillations for Ni/nitrides along with those for Ni and NiO.

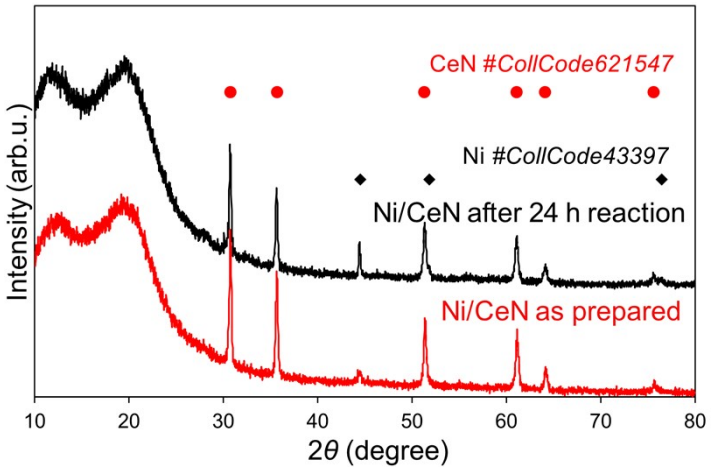

Figure S4. XRD patterns for 10 wt% Ni/CeN as prepared and after 24 h ammonia decomposition reaction at 500°C.

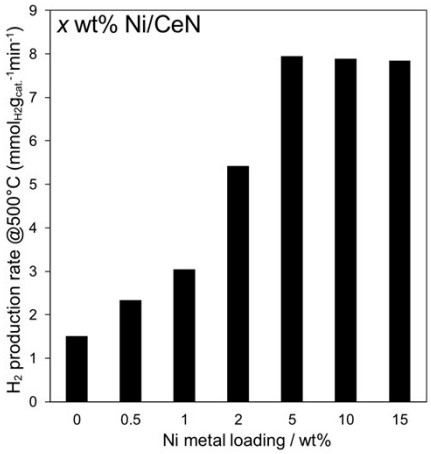

Figure S5. Hydrogen production rate obtained with CeN specimens having various Ni loadings.

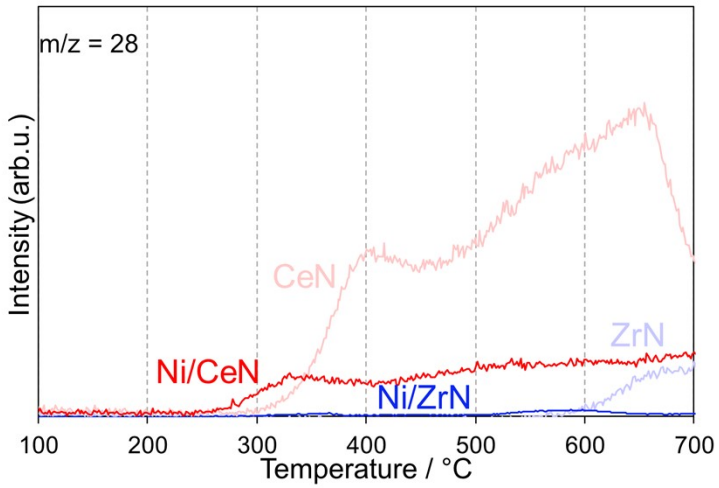

Figure S6. TPD profiles for Ni/CeN and Ni/ZrN under He flow based on monitoring at m/z = 28.

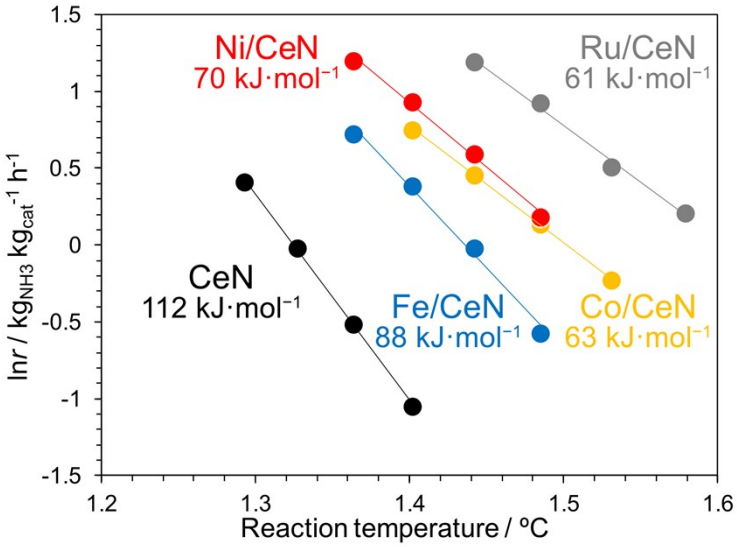

Figure S7. Arrhenius plots for ammonia decomposition over M/CeN (M = Ru, Ni, Co or Fe) below 30% NH3 conversion.

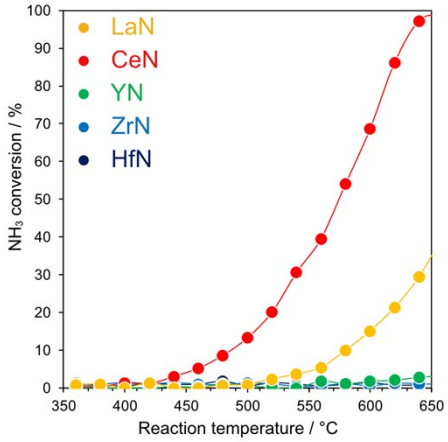

Figure S8. NH_3 conversion during ammonia decomposition over nitrides without metal loading as function of temperature.

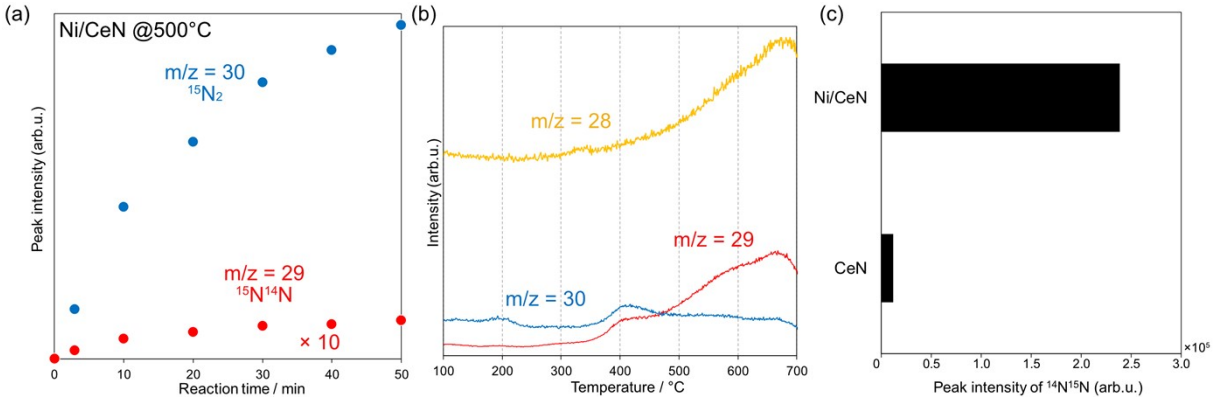

Figure S9. (a) Data from $^{15}NH_3$ decomposition trial using Ni/CeN at 500 °C. (b) N_2-TPD profiles for Ni/CeN after the $^{15}NH_3$ decomposition trial at 500 °C. (c) $^{14}N^{15}N$ produced over 30 min during initial state of $^{15}NH_3$ decomposition over Ni/CeN and CeN.

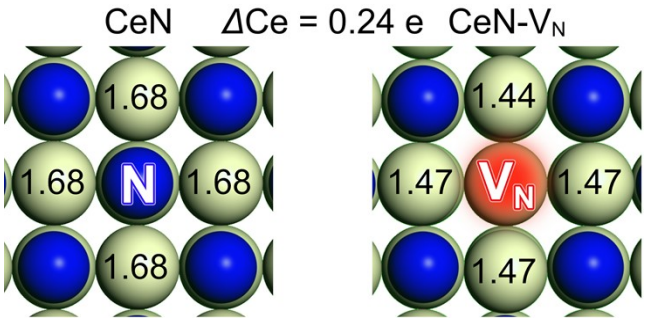

Figure S10. Bader charge analysis of nitride surfaces with V_N formation on CeN (001).

References

1 T.-N. Ye, S.-W. Park, Y. Lu, J. Li, M. Sasase, M. Kitano, T. Tada and H. Hosono, *Nature*, 2020, **583**, 391–395.
2 Y. Lu, J. Li, T. N. Ye, Y. Kobayashi, M. Sasase, M. Kitano and H. Hosono, *ACS Catal.*, 2018, **8**, 11054–11058.
3 G. Kresse and J. Furthmüller, *Phys. Rev. B*, 1996, **54**, 11169–11186.
4 J. P. Perdew, K. Burke and M. Ernzerhof, *Phys. Rev. Lett.*, 1996, **77**, 3865–3868.
5 P. E. Blöchl, *Phys. Rev. B*, 1994, **50**, 17953–17979.
6 G. Kresse and D. Joubert, *Phys. Rev. B*, 1999, **59**, 1758–1775.
7 J. D. Pack and H. J. Monkhorst, *Phys. Rev. B*, 1977, **16**, 1748–1749.
8 S. L. Dudarev, G. A. Botton, S. Y. Savrasov, C. J. Humphreys and A. P. Sutton, *Phys. Rev. B*, 1998, **57**, 1505–1509.
9 P. L. Bramwell, S. Lentink, P. Ngene and P. E. De Jongh, *J. Phys. Chem. C*, 2016, **120**, 27212–27220.
10 W. Zheng, J. Zhang, Q. Ge, H. Xu and W. Li, *Appl. Catal. B Environ.*, 2008, **80**, 98–105.
11 J. Zhang, H. Xu, X. Jin, Q. Ge and W. Li, *Appl. Catal. Gen.*, 2005, **290**, 87–96.
12 H. Liu, H. Wang, J. Shen, Y. Sun and Z. Liu, *Appl. Catal. Gen.*, 2008, **337**, 138–147.
13 X. Li, W. Ji, J. Zhao, S. Wang and C. Au, *J. Catal.*, 2005, **236**, 181–189.
14 T. V. Choudhary, C. Sivadinarayana and D. W. Goodman, *Catal. Lett.*, 2001, **72**, 197–201.
15 S.-F. Yin, Q.-H. Zhang, B.-Q. Xu, W.-X. Zhu, C.-F. Ng and C.-T. Au, *J. Catal.*, 2004, **224**, 384–396.
16 H. Yan, Y.-J. Xu, Y.-Q. Gu, H. Li, X. Wang, Z. Jin, S. Shi, R. Si, C.-J. Jia and C.-H. Yan, *J. Phys. Chem. C*, 2016, **120**, 7685–7696.
17 K. Ogasawara, M. Miyazaki, K. Miyashita, H. Abe, Y. Niwa, M. Sasase, M. Kitano and H. Hosono, *Adv. Energy Mater.*, 2023, **13**, 2301286.
18 K. Ogasawara, T. Nakao, K. Kishida, T.-N. Ye, Y. Lu, H. Abe, Y. Niwa, M. Sasase, M. Kitano and H. Hosono, *ACS Catal.*, 2021, **11**, 11005–11015.
19 F. Chang, H. Wu, R. V. D. Pluijm, J. Guo, P. Ngene and P. E. De Jongh, *J. Phys. Chem. C*, 2019, **123**, 21487–21496.
20 L. I. Osadchaya, V. V. Sokolov, L. N. Trushnikova and A. P. Zubareva, *Inorg. Mater.*, 2003, **39**, 1142–1143.